PCCP

Accepted Manuscript

ROYAL SOCIETY OF CHEMISTRY

www.rsc.org/pccp

Polymer Chemistry

ARTICLE TYPE

Alcohol-soluble bis(*tpy*)thiophenes: new building units for constitutional dynamic conjugated polyelectrolytes

Pavla Štenclová-Bláhová, Jan Svoboda,* Ivana Šloufová, Jiří Vohlídal*

New building units (unimers) for metallo-supramolecular polymers: 2,5-bis(2,2':6',2"-terpyridine-4'-yl)thiophene, **M**, and 5,5'-bis(2,2':6',2"-terpyridine-4'-yl)(2,2'-bithiophene), **B**, with ionic groups attached to thiophene rings are prepared by modification of corresponding bromo-precursors and assembled with Zn^{2+} and Fe^{2+} ions into alcohol-soluble conjugated constitutional-dynamic polyelectrolytes

10 (polyelectrolyte dynamers). Ionization of side groups only slightly affects absorption spectra of unimers as well as dynamers but dramatically changes their solubility. Cyclic conformations of unimer molecules resulting from intramolecular interactions between *tpy* end-groups and cationic or polar (-CH₂Br) side groups are proposed to explain the spectral conformity of the **M**- and **B**-type unimers and their dynamers and also inhibition of the ionization reaction with *tpy* end-groups. The absorption spectra and excitation

15 profiles of Raman spectra show that mainly the red arm of the metal-to-ligand charge transfer band of Fe-dynamers is significantly contributed with transitions involving thiophene rings. The constitutional dynamics of Zn-dynamers is fast while that of Fe-dynamers is so slow that it allows effective separation of the dynamer to fractions in SEC columns. Electronic spectra and viscosity measurements proved that excess of Fe^{2+} ions results in shortening the dynamer chains and their end-capping by these ions.

20 Introduction

Metallo-supramolecular polymers (MSP) are an important subclass of dynamers.[1,2] A molecule of a linear MSP is composed of low-molar-mass or oligomeric units with two chelating end-groups (metal-ion receptors) that enable metal-ion induced

25 reversible self-assembly of the units into chains. Metal ions that facilitate this self-assembly are usually referred to as ion couplers. Depending on the strength of interactions between the end-groups and ion couplers and solubility, molecules of MSPs exhibit constitutional dynamics either at increased temperature, or

30 in solution, or both. The constitutional dynamics gives to MSPs *(i)* processing advantages, *(ii)* responsiveness to external stimuli (adaptability), *(iii)* possibility of tuning the properties or healing structure defects by post-synthesis exchanges of oligomer molecules and/or ion-couplers. The dynamics of MSPs is

35 controlled by the rates of opposite reactions underlying coordination equilibriums, i.e., by the rate of chemical relaxation.
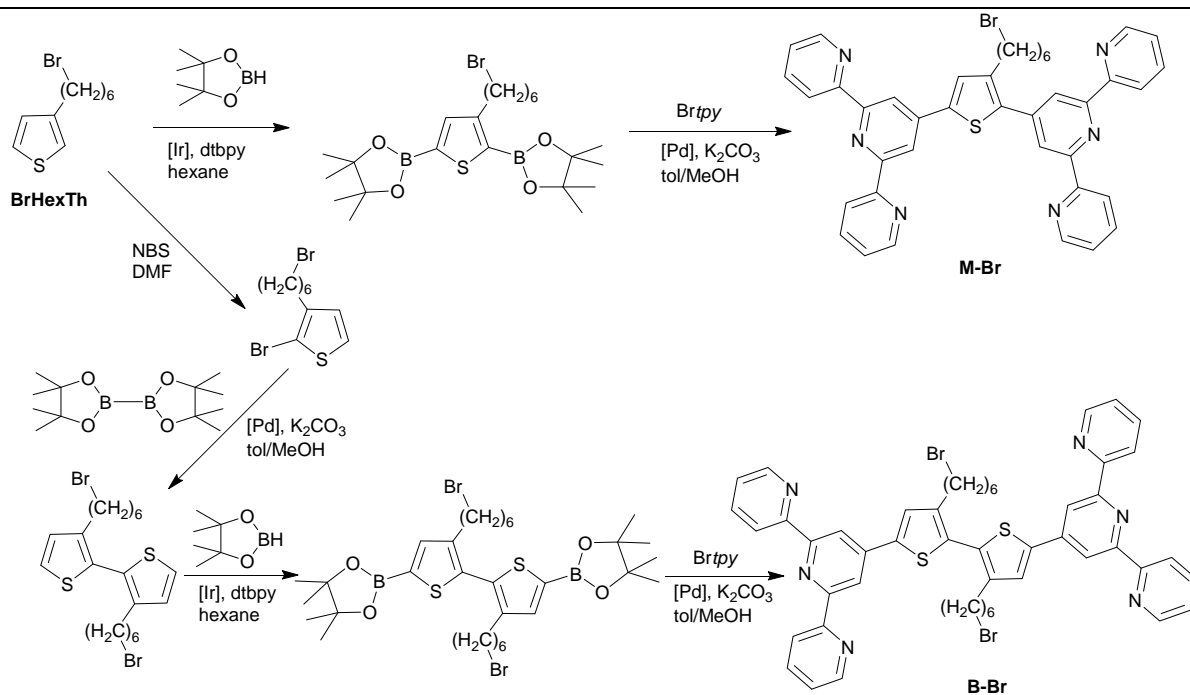
Notes and references

Charles University in Prague, Faculty of Science, Department of Physical and Macromolecular Chemistry, Hlavova 2030, CZ-128 40, Prague 2,
40 *Czech Republic. Fax:+420 224919752; Tel:+420 221951310; E-mail: jan.svoboda@natur.cuni.cz (J. Svoboda), jiri.vohlidal@natur.cuni.cz (J. Vohlídal)*
†Electronic Supplementary Information (ESI) available]. See DOI: 10.1039/b000000x/
45

As the field of dynamers is relatively new, the related terminology has not yet been established, which brings about 50 ambiguity of the term oligomer. Under the dynamics promoting conditions, dynamer molecules are typically composed of only low number of assembled units, most often oligomeric molecules. Such a dynamer is a "superior oligomer" of hierarchically lower oligomer(s). Ambiguity of the term oligomer is thus obvious. 55 Therefore, we use throughout this paper the term *unimer* for an oligomer utilized as a "monomer" in the preparation of a dynamer, as proposed by Ciferri et al.[3]

The MSPs composed of conjugated unimers are of interest as potential materials for devices with applications based on the 60 light/electricity inter-conversion and non-linear optical phenomena (light-emitting devices, photovoltaic cells, etc.).[4–22] High attention has been paid to MSPs derived from conjugated oligomers with tridentate 2,2':6',2"-terpyridine-4'-yl (*tpy*) end units that prefer facial and meridian coordination to metal ions 65 such as Ru^{2+}, Fe^{2+}, Zn^{2+} and Co^{2+}, thus giving well defined linear chains.[20,23–25] However, conjugated MSPs as well as their unimers suffer from poor solubility in solvents suitable for their solution processing. MSPs constituted of bis(*tpy*)oligoarylenes are poorly soluble or insoluble in overwhelming majority of solvents. They 70 are not very best soluble in solvents such as dimethylsulfoxide (DMSO), acetonitrile (AN), or dimethylformamide (DMF), which are not very favorable for preparing good MSP layers.

Chart 1: Structures and codes of prepared unimers and schematic structure of metallo-supramolecular dynamer.

Poor solubility of conjugated linear MSPs originates from rather high stiffness of their chains that strongly supports the inter-chain interactions and suppresses the intra-chain ones. The stiffness of conjugated MSP chains is a logical consequence of their chemical constitution. It mainly stems from two effects: *(i)* increased rigidity of conjugated chains of inbuilt unimers, and *(ii)* ionene structure causing extension of MSP chains due to the electrostatic repulsion between main-chain cations.

An increase in the solubility of conjugated MSPs in medium-polar solvents achieved by introducing pendant alkyl groups to unimeric units[24] is insufficient. Future technologies require materials soluble in "green solvents" such as alcohols and aqueous solutions and in solvents providing good polymer films. Such solubility of conjugated MSPs can be potentially achieved by introducing pendant ionic groups onto unimers. In the present paper, we report on the preparation and basic properties of the ionic unimers of the bis(*tpy*)thiophene type and their transformation into conjugated MSPs by means of coordination to Zn^{2+} and Fe^{2+} ion couplers. These compounds might be classified as conjugated polyelectrolyte dynamers though, according to the molecular structure they are hybrids of polyelectrolytes and ionenes since their chains contain pendent ionic groups as well as charged main chain atoms.[26,27]

Results and discussion

The unimers prepared and studied as well as their abbreviations are shown in **Chart 1**. Metallo-supramolecular dynamers prepared from these unimers are denoted with the prefix $\mathbf{P_{Zn}}$ (dynamers with Zn^{2+} ion couplers) or $\mathbf{P_{Fe}}$ (Fe^{2+} ion couplers) before the unimer label: for example $\mathbf{P_{Zn}M\text{-}Br}$ denotes the dynamer formed from **M-Br** and Zn^{2+} ions; $\mathbf{P_{Fe}B\text{-}N^+}$ the dynamer formed from **B-N$^+$** and Fe^{2+} ions, etc.

Synthesis of unimers and dynamers

Bromohexyl unimers **M-Br** and **B-Br** carrying 6-bromohexyl groups were prepared using the Suzuki-Miyaura coupling strategy (**Scheme 1**) and conditions applied earlier.[28] The key monomer: 3-(6-bromohexyl)thiophene, **BrHexTh**, was prepared by the dropwise addition of 3-thienyllithium to a four-fold stoichiometric excess of 1,6-dibromohexane in hexane and purified by vacuum fractionation. A part of **BrHexTh** was transformed into corresponding 2,5-bis(borolane)[29,30] that was then reacted with Br*tpy* to give unimer **M-Br**. Another portion of **BrHexTh** was brominated with NBS to give 2-bromoderivative that in the reaction with diborolane gave 3,3'-bis(6-bromohexyl)-2,2'-bithiophene. The latter was then transformed to bis(boronate) which, in the reaction with Br*tpy*, gave unimer **B-Br**.

Scheme 1: Preparation of unimers **M-Br** and **B-Br** (precursors of ionic unimers).

Modification of bromohexyl to ionic unimers has surprisingly met serious difficulties. Originally we wanted to replace Br atoms with *N*-methylimidazolium groups - current cations of ionic liquids, since such modification took easily place with poly[3-(2-bromoethoxy)-4-methylthiophene],[31,32] poly(**BrHexTh**),[33] and also on **BrHexTh** even in the presence of free terpyridine in our preliminary experiments. However, in sharp contrast, the reaction of bromo-unimers with *N*-methylimidazole did not proceed at all at laboratory temperature and, at increased temperatures (about 50 °C or higher), significant elimination of HBr took place that gave a considerable fraction of unsaturated hex-5-en-1-yl side groups. The HBr elimination appeared even at the solvent-free conditions: in solutions of **M-Br** or **B-Br** in *N*-methylimidazole at 70 °C. Therefore, we decided to modify **M-Br** or **B-Br** with a stronger agent: trimethylamine (Me₃N), which has one important advantage: its stoichiometric excess is easy to remove by evaporation from the resulting reaction mixture.

The difficulties accompanying the ionization indicate that the reaction of bromohexyl unimers with *N*-methylimidazole is inhibited by *tpy* end-groups. The reason for it might be seen in the increased basicity of *tpy* end-groups due to donation of electrons from neighboring thiophene rings. Interactions between *tpy* and polar –CH₂Br groups can be strong enough to keep these groups in close proximity. This suggests preferred macrocyclic conformations of **B-Br** and **M-Br** molecules since intramolecular cycles are much more resistant to the strain induced by thermal motion compared to linear supramolecular chains. Nevertheless, the intermolecular inhibition with *tpy* end-groups of other molecules is not excluded.

The ¹H NMR spectra evidenced the transformation of bromo- to trimethylammonium- unimers by disappearance of the signal of CH₂(-Br) group (3.38 ppm for **M-Br**; 3.42 ppm for **B-Br**) and appearance of the signal of nine protons of CH₃ group in Me₃N⁺ groups (3.03 ppm for **M-N⁺**; 3.07 ppm for **B-N⁺**). Signal of CH₂ unit linked to -N⁺Me₃ group was not seen being overlaid by the

solvent signal (spectrum taken in methanol). Neither the IR nor the off-resonance Raman spectra provided an additional clear evidence for modification of side groups since, as observed earlier,[24] the bands of thiophene rings and *tpy* end-groups unambiguously dominate in the spectra of unimers.

Metallo-supramolecular dynamers were simply prepared by mixing solutions of a given unimer and zinc or iron(II) perchlorate in the stoichiometric ratio of 1:1 and subsequent evaporating the solvent. Bromohexyl unimers (**M-Br** and **B-Br**) were assembled in the acetonitrile/chloroform (1/1 by vol.) mixed solvent while ionic unimers (**M-N⁺** and **B-N⁺**) in methanol. The ionic unimers as well as dynamers are well soluble in alcohols and sparingly soluble in water wherein, however, the dissolving is a long-lasting process accompanied by fractionation (see Supplementary Info **Figure S1**). This process is the subject of further study.

Optical spectra of unimers and dynamers

The UV/vis absorption spectra of all unimers are very similar each showing a flat band at 280-284 nm, contributed with transitions in *tpy* end groups, and a band at wavelength $\lambda_A = 336$ nm (solutions) or 345 nm (films) belonging to transitions from HOMO that is spread over thiophene rings and central rings of *tpy* groups (**Table 1** and Supplementary Info **Figure S2**). The spectra are similar to the spectrum of **B-H** (unimer with unsubstituted hexyl side groups, $\lambda_A = 339$ nm).[24]

Close similarity of the UV/vis spectra of **Br**- and **N⁺**-unimers is not surprising since the side end-groups are quite distant from main chains. On the other hand, close similarity of the absorption spectra of **M**- and **B**-unimers is not obvious regarding the different numbers of thiophene rings in their chains. The reason for it is a high dihedral angle (ca 67°)[24] of the thiophene-to-thiophene bond in **B**-molecules (due to steric hindrances of side chains – see **Chart 1**), which greatly reduces the delocalization of electrons in **B** chains. Therefore, **B**-type molecules absorb light

like two almost independent 4'-(thiophen-2-yl)terpyridine species.

Tinny difference (6 to 13 nm) between absorption maxima observed for solutions and films proves a negligible effect of the molecular packing on the light absorption by studied unimers. Particularly interesting is the conformity of UV/vis spectra taken from solutions (~ 338 nm) and films (345 ± 1 nm) of **B-Br** and **B-N$^+$**. The parent unimer, **B-H**, namely shows considerable red shift when going from solution (339 nm) to film (410 nm with a shoulder at 450 nm), which proves substantial planarity of **B-H** molecules in the film.[24] Thus the conformity of the solution and solid-state absorption spectra proves to non-planar conformations of **B-Br** and **B-N$^+$** molecules in films. This can be explained by the above-proposed supramolecular macrocyclic conformations of polar and ionic **B**-type molecules, which stabilizes crossing the thiophene ring planes. As above, the disorder owing to analogous intermolecular interactions cannot be excluded. Anyway, these spectral features are consistent with the suggested explanation of the inhibitive effect of *tpy* end groups in ionization of bromoprecursors.

Table 1: Spectroscopic characteristics of prepared unimers and dynamers

Sample	UV/vis absorption λ_A , nm		Luminescence λ_F , nm (ϕ, %)		Stokes shift ν, cm^{-1}	
	solution	film	solution	film	solution	film
Unimers						
M-Br	335	344	406 (3 %)	543 (7 %)	5200	10 650
M-N$^+$	334	347	404 (3 %)	461 (7 %)	5200	7 150
B-Br	338	344	452 (5 %)	561 (4 %)	7450	11 250
B-N$^+$	337	346	450 (5 %)	519 (3 %)	7450	9 650
B-H [a)]	339	400-420 450$_{sh}$	450 (3%)	550	7280	~ 6 000
Zn-dynamers						
P$_{Zn}$M-Br	380	407	440	460 (3 %)	3 600	2 850
P$_{Zn}$M-N$^+$	370	393	444	473 (1 %)	4 500	4 300
P$_{Zn}$B-Br	385	396	550	525 (4 %)	7 800	6 200
P$_{Zn}$B-N$^+$	375	392	550	538 (3 %)	8 500	6 900
P$_{Zn}$B-H [a)]	390	391	535	545	6 950	7 230
Fe-dynamers						
	(λ_{MLCT})	(λ_{MLCT})				
P$_{Fe}$M-Br	325, 373 (590)	394 (608)				
P$_{Fe}$M-N$^+$	325, 370 (588)	388 (601)				
P$_{Fe}$B-Br	322, 370 (594)	386 (598)				
P$_{Fe}$B-N$^+$	320, 366 (591)	380 (598)				

[a)] Data for solutions measured in THF taken from ref.[24]

Unlike the UV/vis absorption, the luminescence emission of **B**-unimers (λ_F = 450 nm) in solutions is significantly red shifted compared to **M**-unimers (λ_F = 405 nm, Supplementary Info **Table S1**), obviously due to the transition of excited **B**-molecules to

lowered-energy conformations with coplanar quinoidal rings and thus more delocalized π-electrons, from which the light emission takes place. The extent of the excited state relaxation of molecules in the solid state is higher than that observed for dissolved molecules as evidenced by the Stokes shift values (**Table 1**). Lowered extent of relaxation observed for the ionic **N$^+$**-type unimers can be attributed to limitations originating from more intense electrostatic interactions.

Absorption spectra of dynamers show the longest wavelength bands red shifted about 30 to 65 nm with respect to the corresponding free unimer, the shift being higher for **Br**-compared to **N$^+$**-dynamers and for Zn- compared to Fe-dynamers. Spectra of Fe-dynamers show an extra band at ca 600 nm (wavelength λ_{MLCT}), which is typical of $(tpy)_2Fe^{2+}$ grouping[34] and is contributed by electronic transitions within the metal to ligand charge transfer (MLCT) complex. As usual, Zn-dynamers derived from $(tpy)_2$ oligomers show luminescence emission while Fe-dynamers not. The absence of luminescence for Fe(II)-dynamers (complexes) is attributed to the fact that their lowest excited state is a *d-d* triplet state that is very close to the ground state.[35] As the potential *d-d* phosphorescence is spin forbidden, the *d-d* triplet state easy depletes the upper excited states and decays by unambiguously preferred non-radiative transitions in accord with the energy gap law.[36,37]

The luminescence emission bands of the solid **P$_{Zn}$M**-dynamers (467±7 nm) are located close to each other as well as the bands of **P$_{Zn}$B**-dynamers (532±7nm). Interestingly, the bands of dissolved dynamers : 442±2 nm for **P$_{Zn}$M**- and 550 nm for **P$_{Zn}$B**-dynamers are not too distant from the bands of solid dynamers. This indicates that the conformational disorder of the dynamer chains in a film is comparable to their disorder in solution.
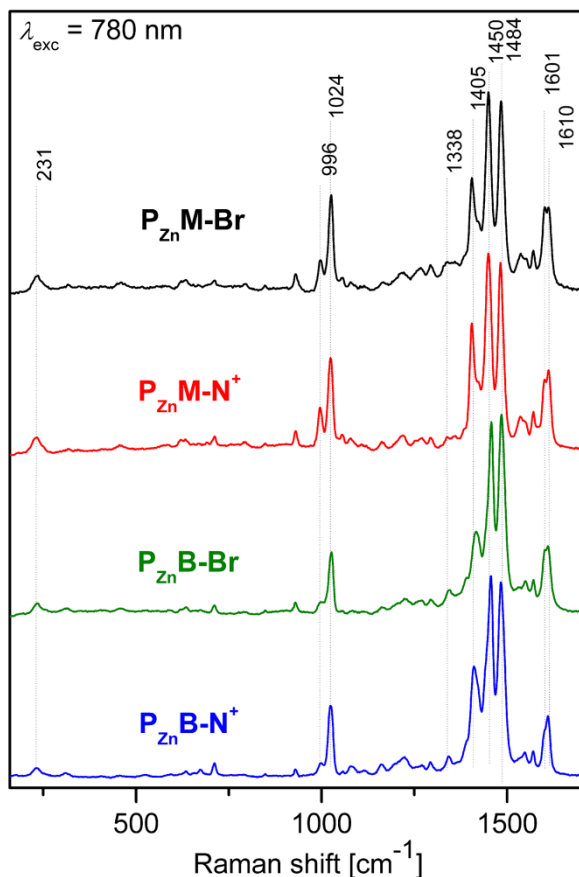
Raman spectra of dynamers

Because Fe-dynamers do not emit luminescence, it was possible to acquire their resonance as well as off-resonance Raman spectra using excitation wavelengths (λ_{ex}) across the whole visible region (λ_{ex} = 445, 532, 633 and 780 nm). In contrast, the spectra of Zn dynamers were measurable only in the off-resonance mode (λ_{ex} = 780 nm) since luminescence dominated the spectra collected with excitations at all others λ_{ex}.

Off-resonance Raman spectra of Zn-dynamers (**Figure 1**) are similar to each other. Each shows a medium to low intensity band of coordinated *tpy* groups: *(i)* ring-stretching modes at 1610 to 1600 cm^{-1}, 1570 cm^{-1} and 1535 to 1548 cm^{-1}, *(ii)* in plane deformation mode at 1288 cm^{-1}, and *(ii)* asymmetric ring breathing mode at about 1025 cm^{-1}.[38,39] However, the strongest bands in these spectra are bands of thiophene-2,5-diyl units,[33,40-43] which appeared at 1484, 1450 and 1405 cm^{-1} for **P$_{Zn}$M**-type dynamers, and at 1484, 1457 and 1411 to 1417 cm^{-1} for **P$_{Zn}$B**-type dynamers. Different end-capping of hexyl-groups has very little impact on the spectral pattern. Thus it can be concluded that the spectral differences primarily stem from different numbers of thiophene rings in unimeric units.

Compared to the spectra of Zn-dynamers, the off-resonance Raman spectra (λ_{ex} = 780 nm) of Fe-dynamers (**Figure 2**) show more intense (and not split into doublet) band of coordinated *tpy* groups at 1610 cm^{-1}, blue-shift of the *tpy* ring-breathing mode band to 1039 cm^{-1}, relatively strong band at 1288 cm^{-1} that should also be attributed to *tpy* groups[38] and somewhat different patterns

of bands attributable to thiophene-rings (1478 to 1345 cm^{-1}). It should be mentioned here that the band at 1478 cm^{-1} is most probably also contributed with transitions in *tpy* groups coordinated to Fe^{2+} ions since Raman spectra of [Fe(terpyridine)$_2$]$^{2+}$ species show a strong band at 1472 cm^{-1}.[38] As can be seen, the spectral differences between **P$_{Fe}$M**-type and **P$_{Fe}$B**-type dynamers are more pronounced compared to differences between their Zn counterparts.

Figure 1: Off-resonance Raman spectra of Zn-dynamers.

Raman spectra of Fe-dynamers taken with different λ_{ex} are compared in **Figure 2**. The spectra of given dynamer differ from each other because each excitation line selectively, resonantly enhances Raman bands of chromophore(s) absorbing at λ_{ex} (Supplementary Info **Figure S2**). Thus the Raman spectra can help to identify chromophore(s) contributing the respective absorption bands.

Raman spectra taken with λ_{ex} = 445 nm showed strong peaks typical of thiophene rings but weak peaks characteristic of *tpy* groups. Moreover, the intensity difference between the *tpy* and thiophene Raman bands of **P$_{Fe}$B**-dynamers is much higher than in the case of **P$_{Fe}$B**-dynamers, which obviously reflects a higher number of thiophene rings in the **B**-type repeating units. Hence it follows that the broad UV/vis band at about 400 nm is mainly contributed with electronic transitions between orbitals spread over the axis of unimer unit that comprises thiophene ring(s).

The excitation at λ_{ex} = 532 nm matches the blue arm of the MLCT band (600 nm). Raman spectra of Fe-dynamers taken with this excitation are the only ones in which overtones and

combination bands are observable in the region from 2200 – 3200 cm^{-1}. Peaks at 1610, 1562, 1537, 1470, 1347 and 1288 cm^{-1} unambiguously dominate the finger-print region of all these resonance Raman spectra, while bands typical of thiophene rings are weak (**Figure 2**). Minor spectral differences between the **M**-type and **B**-type Fe-dynamers are seen in the position of a weak band at 1396 cm^{-1} (**M**-type) vs 1408 cm^{-1} (**B**-type) and the presence of triplet at 682, 673 and 652 cm^{-1} (**M**-type) but only doublet at 681 and 653 cm^{-1} (**B**-type) in the corresponding spectra. Nevertheless, these differences are quite low and do not disturb high similarity of spectral patterns. This extremely large consensus in the spectral patterns is in full concordance with the excitation into the MLCT band of –*tpy*-Fe^{2+}-*tpy*– linkages. However, these spectral patterns significantly differ from the spectral pattern of the resonance Raman spectrum of [Fe(terpyridine)$_2$]$^{2+}$ complex taken with the same excitation: λ_{ex} = 532 nm.[35] This clearly proves that the MLCT state is localized not only on the directly coordinated *tpy* units but also on thiophene unit(s) that are more distant from coordination centre.

Raman spectra taken with λ_{ex} = 633 nm, despite that this line well matches the red arm of the MLCT band, show similar spectral patterns as off-resonance spectra taken with λ_{ex} = 780 nm. Small differences are mainly *(i)* lowered intensity of the doublet (**M**-type) and triplet (**B**-type) in the range 1345-1478 cm^{-1} and *(ii)* increased intensity of the bands at 345 cm^{-1} and in the region from 650 to 800 cm^{-1}. These spectra also differ in the intensity of the band of ring breathing mode (1039 cm^{-1}). However, this band shows rather exceptional trend for all excitations: continuous amplification with increasing λ_{ex}, the trend that has been reported for Raman spectra of various [Ru^{II}(*bpy*)$_3$]$^{2+}$ complexes (*bpy* is 2,2'-bipyridine)[38,44-46] and has remained unexplained.

Important observation is that overtones and combined bands are absent in the spectra excited at 633 nm and their spectral patterns substantially differ from the pattern of spectra excited at 532 nm (**Figure 2**). Regarding that both these excitation lines match the MLCT band one can conclude that the MLCT electronic absorption band of dynamers consists of several different electron transitions of different symmetry.

Assembly of unimers to metallo-supramolecular dynamers

Assembly of dynamers from unimers and metal ions (Mt^{2+}) in solutions (acetonitrile/chloroform 1/1 by vol. for **Br**-type and methanol for **N$^+$**-type unimers and dynamers) was more in detail studied using the UV/vis and fluorescence spectroscopy, viscometry and size exclusion chromatography (SEC).

For spectroscopic studies, a set of solutions of the constant unimer concentration (2·10^{-5} M) and stepwise increasing ions-to-unimer mole ratio ([Mt^{2+}]/[U] = r from 0 to 3) was prepared for each unimer – ions couple. The solutions were allowed to equilibrate for 24 hours prior measuring their UV/vis and luminescence spectra. Changes in the spectra with stepwise increasing composition ratio r are shown in **Figure 3, 4** and Supplementary Info **Figure S5** and **S6**. The UV/vis and luminescence spectral sets are each presented in two figures (except for luminescence spectra of systems with Fe^{2+} ions) in order to show breaks in the development trend, which indicates existence of different stages of assembling. The first break in trend appeared at r slightly above 0.5, the second one, if present, at r > 1.0.
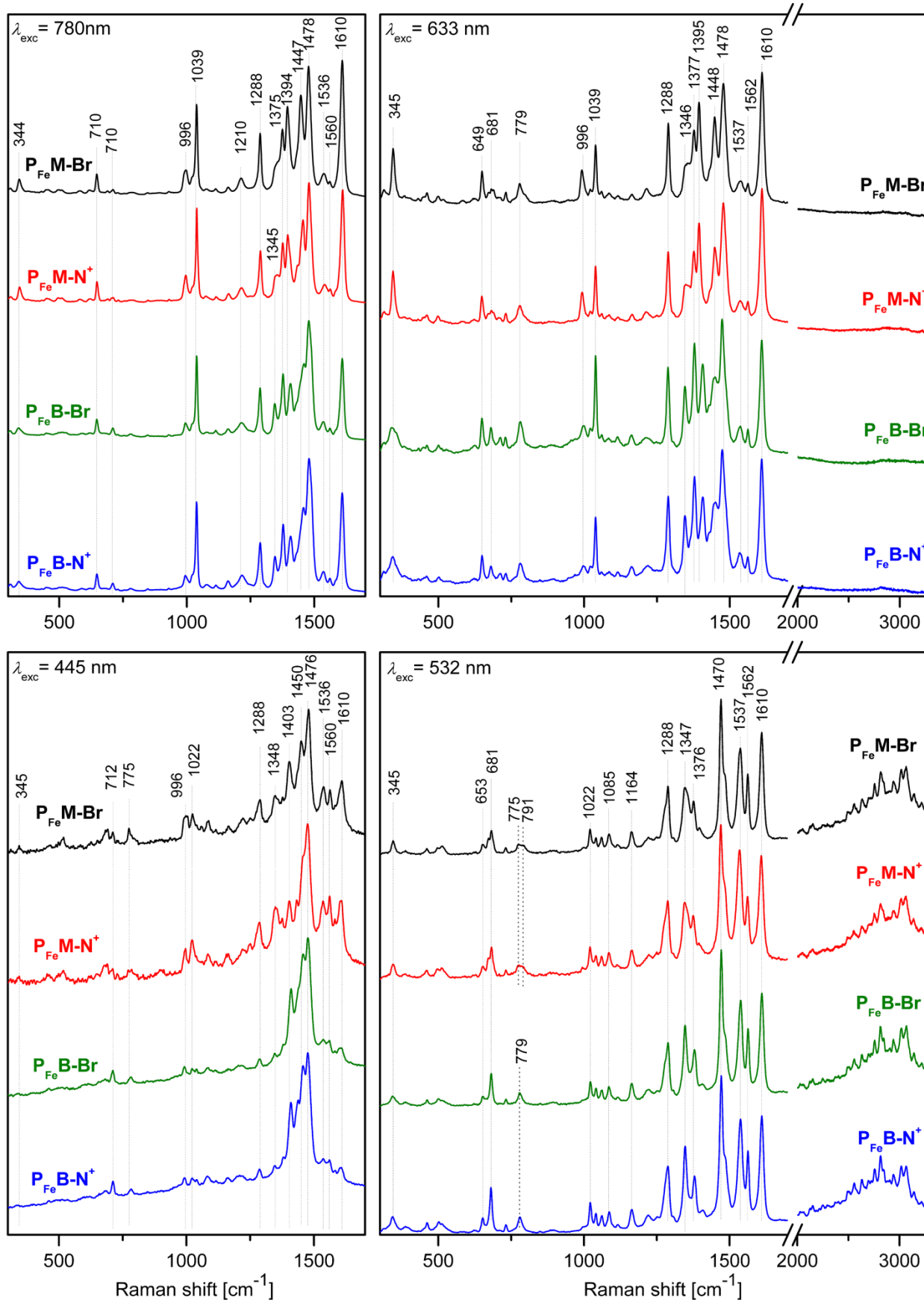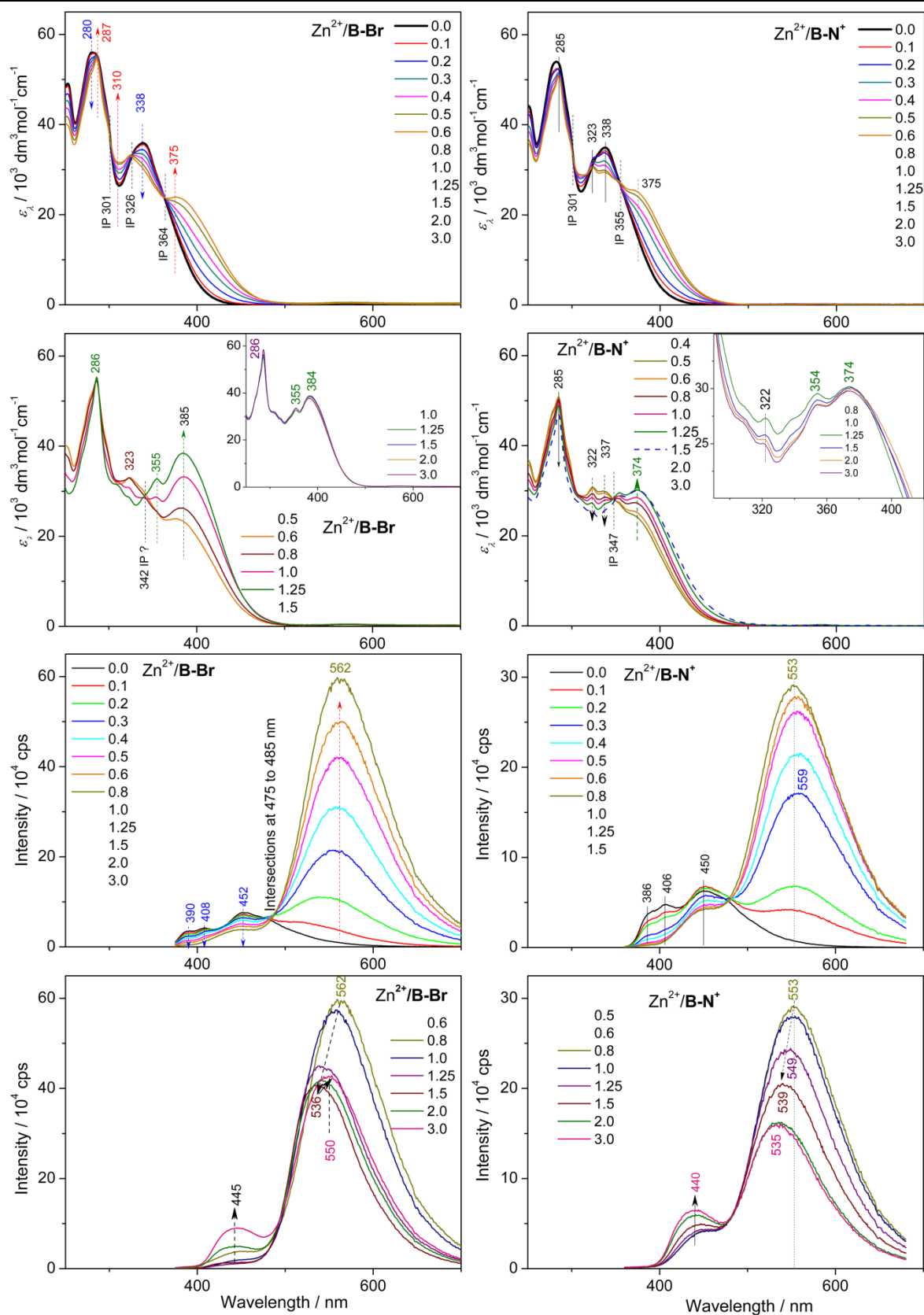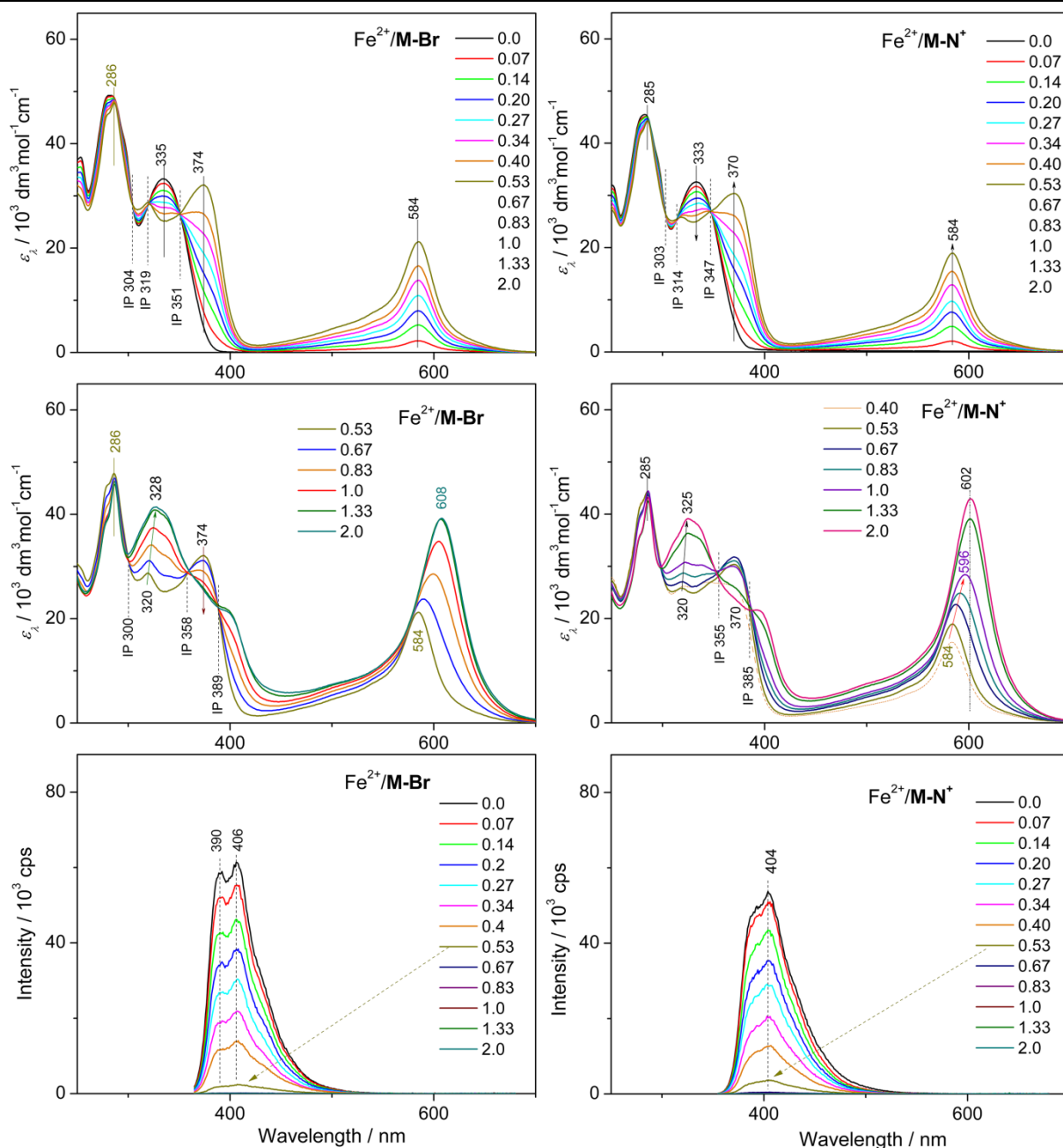
**Figure 2**: Resonance and off-resonance Raman spectra of Fe-dynamers.

Figure 3: Changes in UV/vis and photoluminescence spectra accompanying titration of **B-Br** (left) and **B-N⁺** (right) unimers with Zn^{2+} ions. Initial unimer concentration $2 \cdot 10^{-5}$ mol·dm⁻³; chloroform/acetonitrile (**Br**-unimers), methanol (**N⁺**-unimers), room temperature.

Figure 4: Changes in UV/vis and photoluminescence spectra accompanying titration of **B-Br** (left) and **B-N⁺** (right) unimers with Fe²⁺ ions. Initial unimer concentration $2 \cdot 10^{-5}$ mol·dm⁻³; chloroform/acetonitrile (**Br**-unimers), methanol (**N⁺**-unimers), room temperature.

The first stage of assembling (r from 0 to ca 0.6) is reflected in the UV/vis spectra by: *(i)* small change of the band shape at about 280 nm resulting in the shift of its apex to ca 287 nm, *(ii)* attenuating band at about 336 nm that is typical of free unimer, and *(iii)* appearance of a new band at 370-380 nm. Spectral set of each Mt^{2+}/U system shows two to three isosbestic points (IP), the presence of which indicates transformation of defined free unimer species into another defined species. The stoichiometry says that the newly formed species should be "butterfly dimer" species U-Mt^{2+}-U.

Complementary luminescence spectra of Zn^{2+}/U systems (r from 0 to ca 0.6, **Figure 3**, Supplementary Info **Figure S5**) show a gradually attenuating band of free unimer and simultaneously growing new band of coordinated unimer species. Each spectral set shows one IP, thus supporting the idea on prevailing formation of dimers. On the other hand, luminescence spectra of Fe^{2+}/U systems exhibit only gradually attenuated luminescence to its complete quenching at $r > 0.6$. However, it clearly demonstrates disappearance of free unimer species from solution at $r > 0.6$, and thus as well suggests their preferred conversion to butterfly dimers.

Electronic spectra monitored at r above 0.6, do not pass through IPs characteristic of the first stage, which indicates transition to the second stage of assembly where dynamer chains should grow. Unlike the first stage of assembly, the development of spectral patterns during the second stage is strongly influenced by the structure of unimers. Differences are mainly seen in: *(i)* the extent of amplification of the UV/vis band at 370-380 nm, *(ii)* the presence or absence of new IPs, and *(iii)* spectral patterns in the region from 300 to 400 nm. A direct correlation of the observed differences to the structure of dynamers is not apparent. Nevertheless, all these spectra show either a change in the development trend or almost conservation of the spectral pattern at ratios r above 1.25, which indicates occurrence of the third assembly stage (see **Figure 5** showing the dependence of λ_{MLCT} on r).
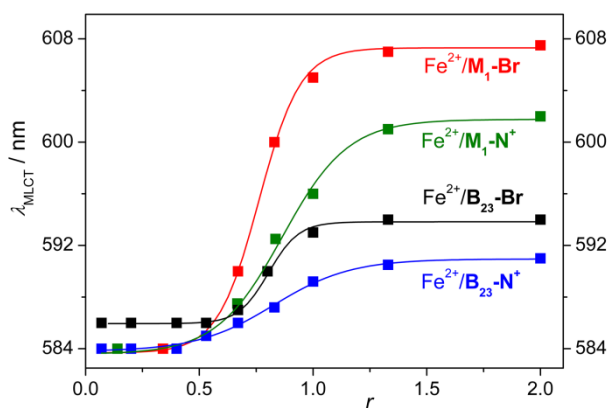
**Figure 5**: The wavelength of MLCT bands of systems with Fe^{2+} ions as a function of the system composition.

The third stage of assembly should consist of the end-capping of dynamer chains with Mt^{2+} ions and depolymerization of the chains to the shorter, also end-caped ones. The reaction of a bis(tpy)Zn^{2+} species with a free Zn^{2+} ion yielding two (tpy)Zn^{2+} species is well known.[47-49] Similar reaction of bis(tpy)Fe^{2+} species, particularly species with monotopic ligands, is not so obvious,[47,50] however, it was reported to take place in the case of metallo-supramolecular polymers.[48,51]
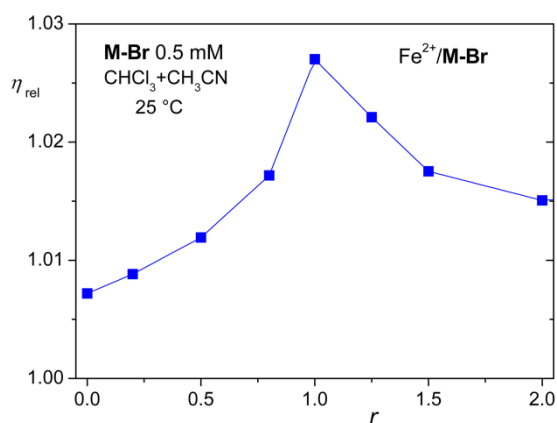
Figure 6: Relative viscosity of solutions of the system Fe^{2+}/**M-Br** as a function of composition.

In order to examine whether this process takes place in solutions of our conjugated dynamers we carried out viscometric study on the system Fe^{2+}/**M-Br** (see results in **Figure 6**). As can be seen, the dependence of the relative viscosity (η_r) of **M-Br** solutions (0.5 mM) in $CHCl_3$/CH_3CN (1:1) on the ratio r passes through maximum at $r = 1$ and then decreases. This indicates that the longest P_{Fe}**M-Br** chains are obtained at $r = 1$ and that these chains most probably depolymerize at $r > 1$. Depolymerization should give the chains end-capped with Fe^{2+} ions.

Assembling of unimers to dynamers was further studied using the SEC instrument equipped with a diode-array UV/vis detector (DAD). Mixed solutions of **M-Br** (0.5 mM) and Zn^{2+} or Fe^{2+} ions (r from 0 to 2.0) in $CHCl_3$/CH_3CN (1:1) mixed solvent were allowed to equilibrate for one day and then injected into the SEC system. The same mixed solvent containing $Bu_4N^+PF_6^-$ (to suppress aggregation) was used as a mobile phase.
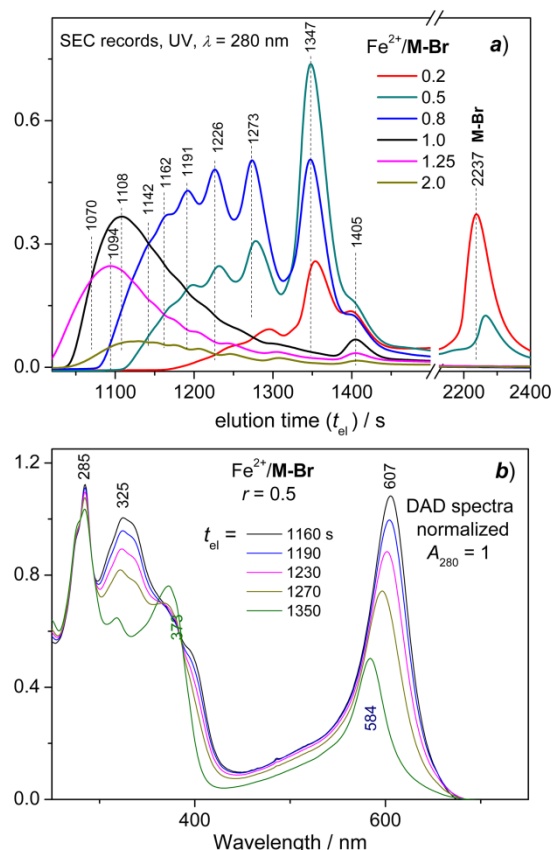
Figure 7: The SEC records of Fe^{2+}/**M-Br** systems of different composition (a) and DAD spectra at different elution time t_{el} (b).

The SEC records of the Zn^{2+}/**M-Br** systems showed only peak of free unimer **M-Br**, which proves a rapid complete dissociation of P_{Zn}**M-Br** chains due to multifold dilution of the solution inside columns (injected 20 μL, elution volume of 37 mL). This proves that P_{Zn}**M-Br** chains are supramolecular systems with rapid constitutional dynamics. In contrast, the Fe^{2+}/**M-Br** systems provided the SEC records typical of polymers, with the resolution decreasing with increasing ratio r (**Figure 7a**). The DAD (i.e., UV/vis) spectra of SEC fractions showed the dependence of the spectral patterns on the elution time (t_{el}): the patterns typical of

long dynamer chains for short t_{el} and typical of butterfly dimers for long t_{el} (**Figure 7b**). This proves that **P$_{Fe}$M-Br** chains are the metallo-supramolecular systems with slow constitutional dynamics. As can be seen, well resolved SEC records were obtained only for systems with $r < 1$. The systems with $r \geq 1$ gave poorly resolved SEC records with the area below elution curve decreasing with increasing value of r, which proves to retention of chains in SEC columns. The detained **P$_{Fe}$M-Br** chains are obviously the chains end-capped with Fe^{2+} ions; they had to be additionally washed out with 2,2'-bipyridine.

The DAD spectra of SEC-fractions (t_{el} = 1350 s) of the systems with $r < 1$ (**Figure 8**) are identical with the dilute solution (0.02 mM) spectrum of dimers. If this SEC peak is assigned to dimers, peak at 1273 s to trimers, etc. (**Figure 7a**), the peak assignment provides linear semi-log dependence of the degree of polymerization (X) of **P$_{Fe}$M-Br** chains on t_{el} for systems with $r < 1$ (Supporting Info **Figure S7**). Average values of X calculated from the SEC records using this calibration are listed in **Table 2**. The used peak assignment is supported by the DAD spectra of higher-X SEC-fractions, which correspond to dilute solution spectra of higher oligomers.
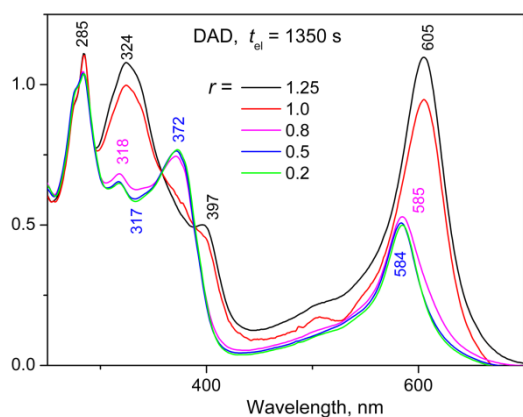

Figure 8: The UV/vis spectra of SEC fractions (t_{el} = 1350 s) of Fe^{2+}/M-Br systems of different composition.

The presence of higher-X fractions in Fe^{2+}/**M-Br** solutions with fairly understoichiometric ratios: r = 0.2 and 0.5 should be ascribed to the effect of transiently locally increased concentration during mixing more concentrated solutions of **M-Br** and Fe^{2+} ions. Formation of dynamer chains is surely a kinetically controlled process which, when mixing twenty five times more concentrated solutions (0.5 mM instead 0.02 mM) should be ca 625 times faster thus giving rise to a high number of longer chains. As the constitutional dynamics of **P$_{Fe}$M-Br** is slow, the initially formed longer chains do not dissociate within one day. On the other hand, the dynamics slowness is luckily since it at all allows SEC analysis of Fe-dynamers (in contrast to Zn-dynamers).

Table 2. Number-average (X_n) and weight-average (X_w) degrees of polymerization of **P$_{Fe}$M-Br** in solution calculated from SEC records.

r	X_n	X_w	Đ
0.2	2.26	2.46	1.09
0.5	2.62	3.10	1.18
0.8	3.31	4.04	1.22
1	5.43	6.62	1.22
1.25	5.94	7.48	1.26

Experimental section

Materials

n-Butyllithium (n-BuLi, 2.5M in hexane), 3-bromothiophene, N-bromosuccinimide (NBS), bis(1,5-cyclooctadiene)di-μ-methoxydiiridium(I) ([Ir(OMe)(COD)]$_2$), 4,4'-di-$tert$-butyl-2,2'-dipyridyl (dtbpy), 4,4,5,5-tetramethyl-1,3,2-dioxaborolane (HBpin), [1,3-bis(2,6-diisopropylphenyl)imidazol-2-ylidene](3-chloropyridyl)palladium(II) dichloride (Peppsi-IPr), bis(pinacolato)diboron (B$_2$pin$_2$), trimethylamine (4.2 M solution in ethanol), zinc perchlorate hexahydrate and iron(II) perchlorate hydrate (all Aldrich), K$_2$CO$_3$, MgSO$_4$ (Lachner) and 4'-bromo-2,2':6'2''-terpyridine (TCI) were used as recieved. Hexane (Lachner) was stored over molecular sieve, tetrahydrofurane (Aldrich) was distilled from LiAlH before use, toluene (Lachner) was distilled from sodium/benzophenone before use, methanol (Aldrich) was bubbled with argon before use, dichloromethane, chloroform (Lachner) and acetonitrile were used as obtained.

Measurements

^{1}H and ^{13}C NMR spectra were recorded on a Varian ^{UNITY}INOVA 400 or Varian SYSTEM 300 instruments in d_8-THF, d_2-CD$_2$Cl$_2$, d-CDCl$_3$ or d_4-CD$_3$OD and referenced to the solvent signal: 7.25 ppm (d-CDCl$_3$), 5.32 ppm (d_2-CD$_2$Cl$_2$), 3.58 ppm (d_8-THF) or 3.31 ppm (d_4-CD$_3$OD) for ^{1}H and 77.0 ppm (d-CDCl$_3$), 53.84 ppm (d_2-CD$_2$Cl$_2$), 67.57 ppm (d_8-THF) or 49.15 ppm (d_4-CD$_3$OD) for ^{13}C spectra. Coupling constants, J (in Hz), were obtained by the first-order analysis. Infrared spectra were recorded on a Thermo Nicolet 7600 FTIR spectrometer equipped with a Spectra Tech InspectIR Plus microscopic accessory using KBr-diluted samples and diffuse reflectance technique (DRIFT) (128 or more scans at resolution 4 cm^{-1}). Raman spectra of solid samples were recorded on a DXR Raman microscope (Thermo Scientific) using excitations across the whole visible region (λ_{ex} = 445, 532, 633 and 780 nm) and usual laser power at the sample from 0.1 to 0.4 mW. UV/VIS spectra were recorded on a Shimadzu UV-2401PC instrument and photoluminescence spectra on a Fluorolog 3-22 Jobin Yvon Spex instrument, using four-window quartz cuvette (1 cm) for solutions and highly oriented pyrolytic graphite (NT-MDT Co., Russia) as substrate for films. The emission spectra were recorded with excitation wavelength, λ_{ex}, matching the absorption maximum of measured compound. Quantum yields, ϕ_F, of photoluminescence were determined by means of a comparison of the integrated spectrum of the compound in question with that of the standard: quinine sulfate diluted solution in 0.5 M H$_2$SO$_4$ (ϕ_F = 0.54; λ_{ex} = 380 nm). Absolute quantum yields for solid samples were measured using

integration sphere Quanta-φ F-3029. Fluorescence decay was monitored with a FluoroHub single photon counting controller on a Fluorolog 3-22 Jobin Yvon Spex instrument using excitation at λ_{ex} = 378 nm for solutions and λ_{ex} = 472 nm for films.
[5] Viscometric measurements were done on a Lovis 2000 M/Me microviscometer (Anton Paar). SEC analyses were done on a Spectra Physics Analytical HPLC instrument fitted with two SEC columns Polymer Labs (Bristol, UK) Mixed-D, Mixed-E and THERMO UV6000 DAD detector. CHCl$_3$+CH$_3$CN (1/1 by vol.)
[10] (CHROMASOLV, Riedel-deHaen) containing Bu$_4$N$^+$PF$_6^-$ (0.05 mol·dm^{-3}) was used as an eluent (0.7 mL/min).

Complexation experiments

In a typical complexation experiment a measured volume of a solution of Zn^{2+} or Fe^{2+} perchlorate (2×10^{-3}M) in CHCl$_3$+CH$_3$CN
[15] (1/1 by vol.) or MeOH was added into a solution of particular unimer in (2×10^{-5}M) in the same solvent. The metal to unimer (Mt^{2+}/U) composition ratio was varied from 0 to 3. The UV/vis absorption and the photoluminescence emission spectra were measured for each solution at room temperature one day after
[20] preparing.

Syntheses of bisterpyridines

2,5-(3-(6-bromohexyl)thiophene-2,5-diyl)bis(4,4,5,5-tetramethyl-1,3,2-dioxaborolane)
To a solution of 3-(6-bromohexyl)thiophene (2.1 g; 8.45 mmol)
[25] in dry hexane (20 mL) [Ir(OMe)(COD)]$_2$ (42 mg, 0.06 mmol) and dtbpy (150 mg, 0.56 mmol) were added. The solution was bubbled with argon and HBpin (4 mL, 3,53 g, 27,6 mmol) was added. The reaction mixture was heated at 50°C for 4 days. Then the mixture was diluted with water (20 mL). After an hour of
[30] stirring in open vessel the solution was extracted with CH$_2$Cl$_2$ (3×50 mL). The organic layer were combined, dried with MgSO$_4$, filtered off and evaporated to get the product as brownish oil. The product was used in following reaction as obtained without further purification. (2.3 g, 4.6 mmol, 55%).
[35] ^{1}H NMR (400 MHz, CDCl$_3$, δ/ppm): 7.50 (s, 1H, Th^4), 3.40 (t, J = 6.8, 2H, Hex^6), 2.87 (t, J = 7.5, 2H, Hex^1), 1.87 – 1.83 (m, 2H, Hex^5), 1.64 – 1.57 (m, 2H, Hex^2), 1.49 – 1.41 (m, 4H, Hex^3+Hex^4), 1.37 – 1.32 (m, 32H, *CH$_3$*-). ^{13}C NMR (101 MHz, CDCl$_3$, δ/ppm): 154.61, 139.46, 84.0, 83.56, 34.0, 32.69, 31.42,
[40] 29.67, 28.28, 27.92, 24.75. ^{11}B NMR (128,3 MHz, CDCl$_3$, δ/ppm): 22.24. FT-IR (cm^{-1}) 3427 (w), 2983 (s), 2940 (s), 2861 (s), 1537 (s), 1483 (s), 1469 (s), 1453 (m), 1396 (s), 1346 (m), 1297 (w), 1275 (w), 1214 (w), 1168 (s), 1152 (s), 1111 (w), 1048 (m), 963 (m), 925 (w), 860 (s), 828 (m), 786 (w), 728 (m), 688
[45] (m), 671 (s), 647 (s), 577 (m), 562 (m), 520 (m), 427 (m). HRMS found m/z: 521.1673 [M$^+$Na]$^+$, C$_{22}$H$_{37}$O$_4$B$_2$BrNaS requires: 521.1674.

2,5-Bis(2,2':6',2''-terpyridine-4'-yl)-3-(6-bromohexyl)thiophene,
[50] *M-Br*
2,5-(3-(6-Bromohexyl)thiophene-2,5-diyl)bis(4,4,5,5-tetramethyl-1,3,2-dioxaborolane) (1.13 g, 2.26 mmol), Br*tpy* (1.47 g, 4.7 mmol), K$_2$CO$_3$ (1.9 g, 13.8 mmol) and Peppsi-IPr (100 mg, 0.15 mmol) were placed in the Schlenk tube and
[55] vacuum was applied. The tube was filled with argon and toluene (16 mL) and methanol (16 mL) were added. The reaction mixture was heated at 88°C overnight. After cooling to room temperature

the mixture was diluted with CH$_2$Cl$_2$ (50 mL) and washed with water (3×150 mL). The organic phase was dried with MgSO$_4$,
[60] filtered off and evaporated. Crude product was dissolved in the smallest amount of THF and hexane was added. After precipitation of white solid the mixture was filtered and the powder was collected. The residual solution was evaporated, dissolved in THF and precipitated again. White powder (0.46 g,
[65] 0.65 mmol, 29 %).
^{1}H NMR (400 MHz, CDCl$_3$, δ/ppm): 8.79 - 8.68 (m, 12H, A^6 + A^3 + B^3), 7.94 – 7.89 (m, 4H, A^4), 7.79 (s, 1H, C^4), 7.42 – 7.37 (m, 4H, A^5), 3.38 (t, J = 6.9, 2H, Hex^6), 2.95 – 2.91 (m, 2H, Hex^1), 1.89 – 1.79 (m, 4H, Hex^2 + Hex^5), 1.49 – 1.46 (m, 2H,
[70] Hex^3 + Hex^4). ^{13}C NMR (101 MHz, CDCl$_3$, δ/ppm): 155.76, 149.14, 143.85, 143.12, 142.19, 141.02, 137.0, 128.98, 123.96, 121.33, 120.55, 117.05, 33.9, 32.70, 30.65, 29.22, 28.52, 27.92. FT-IR (cm^{-1}): 3056 (m), 3011 (m), 2932 (s), 2858 (m), 1597 (s), 1581 (s), 1565 (s), 1467 (s), 1441 (m), 1404 (s), 1310 (m), 1267
[75] (m), 1124 (w), 1095 (w), 1073 (w), 1029 (m), 989 (m), 888 (m), 846 (w), 792 (s), 744 (s), 677 (m), 659 (m), 621 (m), 560 (w), 513 (m). HRMS found m/z: 709.1746 [M$^+$H]$^+$, C$_{40}$H$_{34}$N$_6$BrS requires: 709.1746.

[80] *3,3'-Bis(6-bromohexyl)-2,2'-bithiophene*
2-Bromo-3-(6-bromohexyl)thiophene (1 mL, 1.25 g, 3.84 mmol), B$_2$pin$_2$ (0.48 g, 1.9 mmol), K$_2$CO$_3$ (1.57 g, 11.4 mmol) and Peppsi-IPr (50 mg, 0.07 mmol) were placed into the Schlenk tube and vacuum was applied. After filling the tube with argon,
[85] toluene (15 mL) and methanol (15 mL) were added and the reaction mixture was heated at 90°C for 18 hours. The mixture was cooled down and diluted with CH$_2$Cl$_2$ (50 mL). The solution was washed with water (3×150 mL), dried with MgSO$_4$, filtered off and evaporated. The crude product was purified on column
[90] chromatography (silica, CH$_2$Cl$_2$+hexane 1/1). Yellowish oil (0.34 g, 0.69 mmol, 36%)
^{1}H NMR (400 MHz, CDCl$_3$, δ/ppm): 7.37 (d, J = 5.5, 2H, Th^4), 6.99 (d, J = 5.5, 2H, Th^5), 3.38 (t, J = 6.8, 4H, Hex^6), 2.52 (t, J = 7.8, 4H, Hex^1), 1.82 – 1.75 (m, 4H, Hex^5), 1.61 – 1.53 (m, 4H,
[95] Hex^2), 1.41 – 1.34 (m, 8H, Hex^3+Hex^4). ^{13}C NMR (101 MHz, CDCl$_3$, δ/ppm): 143.04, 129.72, 129.45, 126.56, 34.38, 33.91, 32.71, 31.60, 28.99, 27.93. FT-IR (cm^{-1}): 3101 (w), 3059 (w), 3002 (w), 2932 (s), 2854 (s), 1519 (w), 1460 (m), 1437 (m), 1409 (w), 1371 (w), 1294 (w), 1257 (m), 1232 (m), 1090 (w), 1049
[100] (w), 879 (w), 831 (m), 803 (w), 774 (w), 723 (m), 693 (m), 645 (m), 561 (m). HRMS found m/z: 491.0072 [M$^+$H]$^+$, C$_{20}$H$_{29}$Br$_2$S$_2$ requires: 491.0072.

5,5′-(3,3'-Bis(6-bromohexyl)-2,2'-bithiophene-5,5'-
[105] *diyl)bis(4,4,5,5-tetramethyl-1,3,2-dioxaborolane)*
3,3'-Bis(6-bromohexyl)-2,2'-bithiophene (0.34 g, 0.69 mmol), dtbpy (23 mg, 0.08 mmol) and [Ir(OMe)(COD)]$_2$ (30 mg, 0.04 mmol) were placed in the flask. The flask was flushed with argon and THF (7 mL) and hexane (7 mL) were added. HBpin (0.4 mL,
[110] 0.35 g, 2.76 mmol) was added through septum and the reaction mixture was heated at 55°C for 48 hours. The reaction mixture was diluted with water (20 mL) and stirred in open vessel for an hour. Then the solution was extracted with CH$_2$Cl$_2$ (50 mL). The organic layer was dried with MgSO$_4$, filtered off and evaporated
[115] to get the product as brownish oil. (0.48 g, 0.64 mmol, 93%)
^{1}H NMR (400 MHz, CD$_2$Cl$_2$, δ/ppm): 7.46 (s, 2H, Th^4), 3.37 (t, J

= 7.0, 4H, Hex^6), 2.51 (m, 4H, Hex^1), 1.83 – 1.80 (m, 4H, Hex^5), 1.57 – 1.53 (m, 12H, Hex^2 – Hex^4), 1.33 (s, 32H, CH_3-). ^{13}C NMR (101 MHz, CD$_2$Cl$_2$, δ/ppm): 144.06, 139.25, 84.73, 34.67, 33.30, 30.98, 28.96, 28.44, 26.14, 25.14. ^{11}B NMR (128 MHz, CD$_2$Cl$_2$, δ/ppm): 24.39. FT-IR (cm^{-1}): 3394 (m), 2976 (s), 2931 (s), 2856 (m), 1618 (w), 1530 (m), 1474 (s), 1379 (s), 1330 (s), 1298 (m), 1267 (m), 1214 (w), 1165 (m), 1142 (s), 1027 (m), 982 (m), 961 (w), 925 (w), 852 (s), 802 (m), 727 (w), 665 (m), 577 (w), 519 (w). HRMS found m/z: 765.1595 [M$^+$Na]$^+$, C$_{32}$H$_{50}$O$_4$B$_2$Br$_2$NaS$_2$ requires: 765.1596.

5,5′-Bis(2,2′:6′,2″-terpyridine-4′-yl)-3,3′-di(6-bromohexyl)-2,2′-bithiophene, **B-Br**

5,5'-(3,3'-Bis(6-bromohexyl)-2,2'-bithiophene-5,5'-diyl)bis(4,4,5,5-tetramethyl-1,3,2-dioxaborolane) (0.48 g, 0.64 mmol), Br*tpy* (0.43 g, 1.37 mmol), K$_2$CO$_3$ (0.52 g, 3.76 mmol) and Peppsi-IPr (26 mg, 0.04 mmol) were placed in the Schlenk flask and vacuum was applied. The flask was flushed with argon and toluene (15 mL) and methanol (15 mL) were added. The reaction mixture was heated at 90°C for 18 hours. After cooling to room temperature the reaction mixture was diluted with CH$_2$Cl$_2$ (50 mL) and washed with water (3×100 mL), then dried with MgSO$_4$, filtered off and evaporated. The crude product was purified on column chromatography (aluminium oxide, hexane+THF 3/2). Yellow solid (0.12 g, 0.13 mmol, 20%)
^{1}H NMR (400 MHz, THF, δ/ppm): 8.83 (s, 4H, B^3), 8.72 – 8.70 (m, 8H, A^3+A^6), 7.94 – 7.89 (m, 4H, A^4), 7.87 (s, 2H, C^4), 7.41 – 7.37 (m, 4H, A^5), 3.42 (t, J = 6.8, 4H, Hex^6), 2.77 – 2.74 (m, 4H, Hex^1), 1.89 – 1.79 (m, 8H, Hex^2+Hex^5), 1.51 – 1.38 (m, 8H, Hex^3+Hex^4). ^{13}C NMR (101 MHz, CDCl$_3$, δ/ppm): 156.08, 155.99, 149.12, 143.68, 143.09, 141.51, 136.84, 130.30, 127.45, 123.90, 121.32, 116.81, 33.88, 32.68, 30.49, 29.01, 28.51, 27.95. FT-IR (cm^{-1}): 3057 (w), 3010 (w), 2930 (m), 2854 (m), 1597 (m), 1581 (s), 1565 (s), 1528 (w), 1466 (m), 1443 (m), 1419 (w), 1403 (m), 1382 (w), 1360 (w), 1263 (m), 1209 (w), 1147 (w), 1123 (w), 1094 (m), 1072 (m), 1018 (m), 989 (m), 959 (w), 901 (w), 881 (m), 847 (m), 791 (s), 773 (m), 746 (m), 734 (m), 688 (w), 677 (w), 658 (m), 648 (w), 633 (w), 621 (w), 507 (w). HRMS found m/z: 953.1673 [M$^+$H]$^+$, C$_{50}$H$_{47}$N$_6$Br$_2$S$_2$ requires: 953.1665.

Quarternization

A weighed amount of a given Br-unimer was dissolved in THF (conc. 4×10^{-3}M), trimethylamine was added (10eq.) as ethanol solution (4.2 M) and the mixture was kept at 25°C for four days. The precipitated product was isolated by centrifugation, washed with THF and dried in vacuum.

6-[2,5-Bis(2,2′:6′,2′′-terpyridine-4′-yl)thiophene-3-yl]hexan-1-yl trimethylammonium bromide, **M-N$^+$**
Yellowish powder 37 %. ^{1}H NMR (400 MHz, CD$_3$OD, δ/ppm): 8.70 – 8.69 (m, 4H, A^6), 8.64 – 8.60 (m, 6H, A^3 + B^3 or B$^{3'}$), 8.54 (s, 2H, B^3 or B$^{3'}$), 8.01 – 7.96 (m, 4H, A^4), 7.80 (s, 1H, C^4), 7.49 – 7.45 (m, 4H, A^5), 3.25 – 3.20 (m, 2H, Hex^6) 3.03 (s, 9H, N-(CH_3)$_3$), 2.98 (t, J = 7.6, 2H, Hex^1), 1.87 – 1.72 (m, 4H, Hex^5 + Hex^2), 1.54 – 1.50 (m, 2H, Hex^4), 1.42 – 1.38 (m, 2H, Hex^3). ^{13}C NMR (101 MHz, CD$_3$OD, δ/ppm): 157.74, 157.61, 157.20, 150.66, 145.41, 144.51, 139.06, 130.85, 126.0, 123.15, 121.48,

117.93, 68.14, 53.78, 31.73, 30.13, 27.47, 27.45, 24.20. FT-IR (cm^{-1}): 3412 (m), 3055 (m), 3012 (m), 2940 (s), 2861 (m), 1767 (w), 1722 (m), 1597 (s), 1582 (s), 1557 (s), 1468 (s), 1441 (m), 1403 (s), 1381 (m), 1266 (m), 1168 (w), 1126 (w), 1095 (w), 1073 (m), 1031 (m), 989 (m), 966 (w), 888 (m), 846 (w), 793 (s), 745 (s), 677 (m), 660 (m), 621 (w), 589 (w), 569 (w), 513 (m), 502 (w), 471 (w). HRMS found m/z: 688.3218 [M$^+$H]$^+$, C$_{43}$H$_{42}$N$_7$S requires: 688.3217.

6,6′-[5,5′-Bis(2,2′:6′,2′′-terpyridine-4′-yl)-2,2′-bithiophene-3,3′-diyl]bis[hexan-1,1′-diyl trimethylammonium]bromide, **B-N$^+$**
Orange powder 41 %. ^{1}H NMR (400 MHz, CD$_3$OD, δ/ppm): 8.72 – 8.71 (m, 4H, A^6), 8.62 – 8.59 (m, 4H, A^3), 8.56 (s, 4H, B^3), 8.01 (td, J = 7.7, J = 1.6, 4H, A^4), 7.8 (s, 2H, C^4), 7.53 – 7.50 (ddd, J = 7.4, J = 4.8, J = 1.3, 4H, A^5), 3.31 – 3.28 (m, 4H, Hex^6), 3.07 (s, 18H, N-(CH_3)$_3$), 2.74 (t, J = 7.7, 4H, Hex^1), 1.83 – 1.75 (m, 8H, Hex^5 + Hex^2), 1.53 – 1.30 (m, 8H, Hex^3 + Hex^4) ^{13}C NMR (101 MHz, CD$_3$OD δ/ppm): 157.82, 157.67, 157.22, 150.47, 144.68, 139.25, 139.14, 132.09, 129.53, 126.11, 123.30, 117.82, 68.19, 53.76, 31.78, 30.24, 27.49, 26.07, 24.25. FT-IR (cm^{-1}): 3404 (s), 3058 (m), 3015 (m), 2933 (s), 2858 (m), 1722 (s), 1674 (s), 1584 (s), 1567 (s), 1469 (s), 1402 (s), 1265 (m), 1210 (m), 1176 (w), 1124 (w), 1094 (w), 1072 (m), 1044 (w), 1018 (m), 991 (m), 971 (w), 907 (w), 886 (m), 846 (m), 792 (s), 743 (s), 659 (s), 622 (s), 586 (w), 573 (w), 529 (m), 507 (w), 490 (w), 457 (w), 430 (w). HRMS found m/z: 456.2343 [M$^+$H]$^{2+}$, C$_{56}$H$_{64}$N$_8$S$_2$ requires: 456.2342.

Conclusions

The here exploited route to alcohol-soluble ionic unimers includes preparation of their ω-bromoalkyl precursors, which is not too easy but already well mastered procedure, and replacing terminal bromine atoms with ammonium type groups. An inverse approach, coupling of ionic thiophenes with Br-*tpy*, is difficult owing to diverse solubility of reactants, catalyst and auxiliary base. Though the modification of bromo-unimers to the ionic ones seems trivial, it is inhibited by *tpy* end-groups and, therefore, is well feasible only with highly reactive amines.

Spectroscopic study of unimers' assembly with metal ions in dilute solutions provided the UV/vis and luminescence spectral patterns characteristic of the U-Mt^{2+}-U type dimers, dynamer chains with free *tpy* end-groups and dynamer chains capped with metal ions. Absorption spectra of SEC fractions of non-ionic Fe-dynamer **P$_{Fe}$M-Br** well agree with the dilute solution spectra of the systems with corresponding composition ratios *r*. The SEC study further proved that the constitutional dynamics of Zn-dynamers is fast while that of Fe-dynamers slow. It also provided a good calibration dependence, which allowed determining the average values of the degree of polymerization of the dynamer in solutions; this characteristic of dynamers is otherwise almost not accessible and is the subject of the question after almost every conference presentation. Unfortunately, the ionic Fe-dynamers were not effectively separated in SEC columns due to the strong interference of the adsorption mode.

Relative stability of Fe-dynamer chains in solutions (changes lasting for two months are reported in the literature)[48] should be attributed to the MLCT within the *tpy*-Fe^{2+}-*tpy* linkages. The here

presented UV/vis spectra as well as the spectra presented earlier[47,50,52] confirm that the MLCT bands are contributed also with transitions within central blocks of unimeric units. The resonance Raman spectra obtained in this study indicate that the transitions within central block significantly affect the longer-wavelength part of the MLCT band while its shorter-wavelength arm is mainly contributed with transitions within *tpy* end-groups.

Acknowledgement

References

1   J. Lehn, *Prog. Polym. Sci.*, 2005, **30**, 814.
2   J. W. Steed and J. L. Atwood, *Supramolecular chemistry, 2nd edition ed.*, John Wiley & Sons, Ltd., 2009.
3   Ciferri in *Supramolecular Polymers, 2nd edition*, ed. by Ciferri, CRC Press, 2005.
4   M. Beley, D. Delabouglise, G. Houppy, J. Husson and J.-P. Petit, *Inorganica Chim. Acta*, 2005, **358**, 3075.
5   A. Wild, F. Schlütter, G. M. Pavlov, C. Friebe, G. Festag, A. Winter, M. D. Hager, V. Cimrová, U. S. Schubert, *Macromol. Rapid Commun.*, 2010, **31**, 868.
6   A. El-Ghayoury, A. P. H. J. Schenning and E. W. Meijer, *J. Polym. Sci. Part A Polym. Chem.*, 2002, **40**, 4020.
7   A. Harriman, G. Izzet, S. Goeb, A. De Nicola and R. Ziessel, *Inorg. Chem.*, 2006, **45**, 9729.
8   S. C. Yu, C. C. Kwok, W. K. Chan and C. M. Che, *Adv. Mater.*, 2003, **15**, 1643.
9   P. R. Andres and U. S. Schubert, *Adv. Mater.*, 2004, **16**, 1043.
10 A. Barbieri, B. Ventura, F. Barigelletti, A. De Nicola, M. Quesada and R. Ziessel, *Inorg. Chem.*, 2004, **43**, 7359.
11 Q. Wu, J. Wang, H. Hu, Y. Shangguan, F. Fu, M. Yang, F. Dong and G. Xue, *Inorg. Chem. Commun.*, 2011, **14**, 484.
12 R. Siebert, A. Winter, M. Schmitt, J. Popp, U. S. Schubert and B. Dietzek, *Macromol. Rapid Commun.*, 2012, **33**, 481.
13 R. Dobrawa, M. Lysetska, P. Ballester, M. Grüne and F. Würthner, *Macromolecules*, 2005, **38**, 1315.
14 F. S. Han, M. Higuchi, Y. Akasaka, Y. Otsuka and D. G. Kurth, *Thin Solid Films*, 2008, **516**, 2469.
15 P. D. Vellis, J. A. Mikroyannidis, C. Lo and C. Hsu, *J. Polym. Sci. Part A Polym. Chem.*, 2008, **46**, 7702.
16 Y. Chen and H. Lin, *J. Polym. Sci. Part A Polym. Chem.*, 2007, **45**, 3243.
17 A. Winter, C. Friebe, M. Chiper, M. D. Hager and U. S. Schubert, *J. Polym. Sci. Part A Polym. Chem.*, 2009, **3**, 4083.
18 F. Barigelletti and L. Flamigni, *Chem. Soc. Rev.*, 2000, **29**, 1.
19 M. Chiper, R. Hoogenboom and U. S. Schubert, *Macromol. Rapid Commun.*, 2009, **30**, 565.
20 A. Maier, K. Cheng, J. Savych and B. Tieke, 2011, **3**, 2710.
21 A. Wild, A. Teichler, C.-L. Ho, X.-Z. Wang, H. Zhan, F. Schlütter, A. Winter, M. D. Hager, W.-Y. Wong and U. S. Schubert, *J. Mater. Chem. C*, 2013, **1**, 1812.
22 Y. Li, T. Ren and W.-J. Dong, *J. Photochem. Photobiol. A Chem.*, 2013, **251**, 1.
23 R. Siebert, Y. Tian, R. Camacho, A. Winter, A. Wild, A. Krieg, U. S. Schubert, J. Popp, I. G. Scheblykin and B. Dietzek, *J. Mater. Chem.*, 2012, **22**, 16041.
24 P. Bláhová, J. Zedník, I. Šloufová, J. Vohlídal and J. Svoboda, *Soft Mater.*, 2014, **12**, 214.
25 L. Fillaud, G. Trippé-Allard and J. C. Lacroix, *Org. Lett.*, 2013, **15**, 1028.
26 M. Barón, K.-H. Hellwich, M. Hess, K. Horie, A. D. Jenkins, R. G. Jones, J. Kahovec, P. Kratochvíl, W. V. Metanomski, W. Mormann, R. F. T. Stepto, J. Vohlídal and E. S. Wilks, *Pure Appl. Chem.*, 2009, **81**, 1131.
27 M. Hess, R. G. Jones, J. Kahovec, T. Kitayama, P. Kratochvil, P. Kubisa, W. Mormann, R. F. T. Stepto, D. Tabak, J. Vohlidal and E. S. Wilks, *Pure Appl. Chem.*, 2006, **78**, 2067.
28 J. Svoboda, P. Stenclova, F. Uhlík, J. Zedník and J. Vohlídal, *Tetrahedron*, 2011, **67**, 75.
29 G. a Chotana, V. a Kallepalli, R. E. Maleczka and M. R. Smith, *Tetrahedron*, 2008, **64**, 6103.
30 T. Ishiyama, Y. Nobuta, J. F. Hartwig and N. Miyaura, *Chem. Commun,* 2003, 2924.
31 H. a. Ho and M. Leclerc, *J. Am. Chem. Soc.*, 2003, **125**, 4412.
32 F. Le Floch, H.-A. H. a. Ho, P. Harding-Lepage, M. Bédard, R. Neagu-Plesu and M. Leclerc, *Adv. Mater.*, 2005, **17**, 1251.
33 D. Bondarev, J. Zedník, I. Šloufová, A. Sharf, M. Procházka, J. Pfleger and J. Vohlídal, *J. Polym. Sci. Part A-Polymer Chem.*, 2010, **48**, 3073.
34 U. S. Schubert, H. Hofmeier and G. R. Newkome, *Modern Terpyridine Chemistry*, Wiley-VCH Verlag GmbH, Weinheim, 2006.
35 J. N. Demas and B. A. DeGraft in: *Topics in Fluorescence Spectroscopy: Volume 4: Probe Design and Chemical Sensing* (J. R. Lakowicz, Ed.), Springer Science & Business Media 1994, Chapter 4.5, p. 81.
36 R. Englman and J. Jortner, *Mol. Phys.,* 1970, **18**, 145.
37 R. Siebert, A. Winter, M. Schmitt, J. Popp, U. S. Schubert and B. Dietzek, *Macromol. Rapid Commun.*, 2012, **33**, 481.
38 I. Šloufová, B. Vlčková, M. Procházka, J. Svoboda and J. Vohlídal, *J. Raman Spectrosc.*, 2014, **45**, 338.
39 R. Horvath, J. Lombard, J.-C. Leprêtre, M.-N. Collomb, A. Deronzier, J. Chauvin and K. C. Gordon, *Dalton Trans.*, 2013, **42**, 16527.
40 S. Kazim, J. Pfleger, K. Halašová, M. Procházka, D. Bondarev and J. Vohlídal, *Eur. Phys. J. Appl. Phys.*, 2011, **55**, 23905.
41 S. Kazim, J. Pfleger, M. Procházka, D. Bondarev and J. Vohlídal, *J. Colloid Interface Sci.*, 2011, **354**, 611.
42 E. A. Bazzaoui, M. Bazzaoui, J. Aubard, J. S. Lomas, N. Félidj and G. Lévi, *Synth. Met.*, 2001, **123**, 299.
43 K. Mukherjee, D. Bhattacharjee and T. Misra, *J. Colloid Interface Sci.*, 1999, **213**, 46.
44 I. Srnova-Šloufová, B. Vlčková, T. L. Snoeck, D. J. Stufkens and P. Matějka, *Inorg. Chem.*, 2000, **39**, 3551.
45 P. K. Mallick, G. D. Danzer, D. P. Strommen and R. Kincaid, James, *J. Phys. Chem.*, 1988, **92**, 5628 .
46 D. P. Strommen, P. K. Mallick, G. D. Danzer, R. S. Lumpkin and R. Kincaid, James, *J. Phys. Chem.*, 1990, **94**, 1358.
47 T. Vitvarová, J. Zedník, M. Bláha, J. Vohlídal and J. Svoboda, *Eur. J. Inorg. Chem.*, 2012, **2012**, 3866.
48 G. Schwarz, I. Haßlauer and D. G. Kurth, *Adv. Colloid Interface Sci.*, 2014, **207**, 107.
49 V. Stepanenko, M. Stocker, P. Müller, M. Büchner and F. Würthner, *J. Mater. Chem.*, 2009, **19**, 6816.
50 R. A. Dobrawa, *Ph.D. Thesis*, Bayerischer Julius-Maximilians-Universität Würzburg, 2004.
51 G. Schwarz, Y. Bodenthin, T. Geue, J. Koetz and D. G. Kurth, *Macromolecules*, 2010, **43**, 494.
52 R. Dobrawa and F. Würthner, *J. Polym. Sci. Part A Polym. Chem.*, 2005, **43**, 4981.